Simulation of Two-Body Interaction in Waves with the Immersed Boundary Method

Wei Meng and Wei Qiu*

Department of Ocean and Naval Architectural Engineering
Memorial University, St. John's, NL, Canada
∗ Email: qiuw@mun.ca

1 Introduction

Hydrodynamic interactions between multiple floating bodies in a close proximity continue to be of concern for design and operation of marine structures. Potential-flow based methods have been widely employed to solve the problem of multiple body interaction in waves. However, artificial damping has to be input to suppress the unrealistic prediction of wave elevation in the gap. For example, Huijsmans et al. (2001), Newman (2003) and Chen (2004) used different methods by including artificial damping. Recently, studies based on CFD methods have been carried out to consider the viscous effect in two-body interactions. For instance, Ok et al. (2017) simulated motions of vessels floating side by side using the Arbitrary Lagrangian–Eulerian (ALE) solver in OpenFOAM. However, the ALE method was inadequate to handle large relative body motions since meshes between bodies are suppressed or stretched, causing instabilities in the simulations.

In the present study, an immersed boundary method has been developed to solve multi-body interactions on the Cartesian grids based on the finite volume solver in OpenFOAM. A level-set method is employed to determine the immersed boundaries. The free surface is captured using the geometrical Volume-of-Fluid (VOF) method (Roenby et al., 2016). Incoming waves are generated using the waves2Foam toolbox (Jacobsen et al, 2012). Numerical simulations were carried out for two floating bodies with soft moorings in head seas and numerical results are compared with model test data (Qiu et al., 2019).

2 Numerical Methods

The multi-phase incompressible viscous flow, involving water, air and solid, is governed by the momentum equations and the continuity equation:

$$\frac{\partial(\rho \mathbf{U})}{\partial t} + \nabla \cdot (\rho \mathbf{U}\mathbf{U}) - \nabla \cdot [\mu(\nabla \mathbf{U} + \nabla \mathbf{U}^T)] = -\nabla p + \rho \mathbf{g} \tag{1}$$

$$\nabla \cdot \mathbf{U} = 0 \tag{2}$$

where $\mathbf{U}$ is the fluid velocity, ρ is the density, μ is the dynamic viscosity, p is the pressure, and $\mathbf{g}$ is the gravitational acceleration. It is noted that surface tension is not considered in the present work.

Prior to solving the governing equations for the fluids, the transport equations for volume fractions of three phases, α_m, are solved based on the divergence-free velocity field computed from the previous time step and positions of rigid bodies:

$$\frac{\partial \alpha_m}{\partial t} + \nabla \cdot (\mathbf{U}\alpha_m) = 0 \tag{3}$$

where $m = 1, 2, 3$ represent the water, air and solid phases, respectively.

The governing equations are discretized using the finite volume method (FVM). The Pressure Implicit with Splitting of Operators (PISO) algorithm is applied for the velocity-pressure coupling, in which the pressure Poisson equation is solved for a few times to enforce the continuity equation. It is noted that the velocities are

stored on both cell centres, denoted as $\mathbf{U}$, and face centres, denoted as $\mathbf{U}_f$, in OpenFOAM, and it is U_f that strictly satisfies the continuity equation.

The no-flux and no-slip velocity boundary conditions are imposed on immersed boundaries and are enforced in each PISO loop before solving the pressure Poisson equation. When a computational cell or face is cut by or lies within an immersed boundary, velocities at this location are modified based on body motions and the cell volume fraction, α_3, and the face area fraction, α_{3f}, of the solid phase, i.e.,

$$\mathbf{U}' = \alpha_3 \mathbf{U}_{IB} + (1 - \alpha_3)\mathbf{U} \qquad (4)$$

$$\mathbf{U}'_f = \alpha_{3f} \mathbf{U}_{IBf} + (1 - \alpha_{3f})\mathbf{U}_f \qquad (5)$$

where $\mathbf{U}_{IB}$ and $\mathbf{U}_{IBf}$ are velocities of the cell and the face, respectively, based on the rigid body motions, and $\mathbf{U}$ and $\mathbf{U}_f$ are those computed by solving the governing equations.

When a cell or a face is located inside of a rigid body, the corresponding volume and face fractions are set to 1. When it is cut by an immersed boundary, the fractions are calculated by using a level set function, $\varphi(\mathbf{x})$, which is defined at a cell vertex to identify an immersed boundary. When a vertex lies in the solid region, $\varphi(\mathbf{x})$ is negative; otherwise positive. The immersed boundaries are located at $\varphi(\mathbf{x}) = 0$. When values of $\varphi(\mathbf{x})$ at vertices of a cell or face are in different signs, it means the cell or face is cut by an immersed boundary, as shown in Fig. 1. Furthermore, the intersection points between an immersed boundary and cell edges are obtained by linear interpolations. The fractions of the solid phase can then be calculated by decomposing the remaining cell or face into pyramids or triangles and summing their corresponding fraction values.
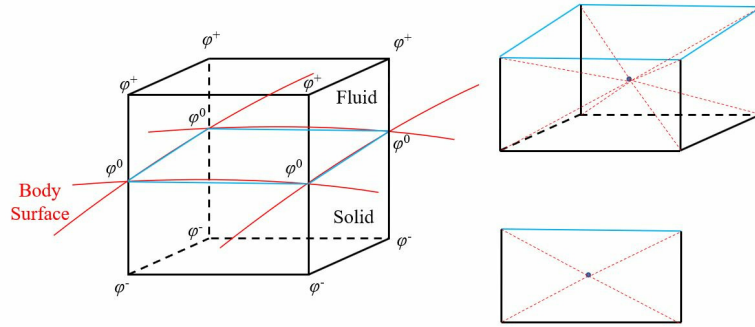
Figure 1: Cell and Face Cut by an Immersed Boundary

The geometrical VOF method based toolbox, IsoAdvector (Roenby et al, 2016), is employed for the advection of water-air interface, i.e. to solve the transport equation for the volume fraction of the water phase, α_1. A geometrical surface reconstruction is first performed based on the α_1 values. The volumes of water transported across faces of cells are then calculated by accounting for the movement of the reconstructed free surfaces within a time step. This method maintains the sharpness of interface and the conservation of mass, thus it is suitable for long-duration simulations such as two-body interactions in waves.

The wave generation toolbox, waves2Foam (Jacobsen et al., 2012), is used for the wave modeling. An inlet relaxation zone and an outlet wave damping zone are employed to avoid the reflected waves from the wave maker boundary and the outlet boundary. In the present study, the inlet relaxation zone, the computational zone and the outlet wave damping zone are set as $1.0L$, $3.0L$, and 3.0λ, respectively, where L is the ship length and λ is the wave length.

3   Results and Discussion

Preliminary numerical simulations were carried out for two models in two regular waves: a long incident wave with wave frequency of $\omega = 4.27 rad/s$ (model scale) and $\lambda/L = 1.69$ and a shorter one with $\omega = 7.16 rad/s$ and $\lambda/L = 0.60$. The model length, L, is $2m$. The numerical settings, including the tank width and depth, gap ($0.4m$), mooring layout and model mass properties, are the same as those for the experimental tests in the towing tank of Memorial University (Qiu et al., 2019). Figure 2 presents the computational domain and associated boundary conditions. The computed motions of two bodies and wave elevations in the gap are compared with the experimental results. About 8.4M and 7.8M Cartesian grids were used for the long and short wave cases, respectively, and 120 grids were distributed per wave length.
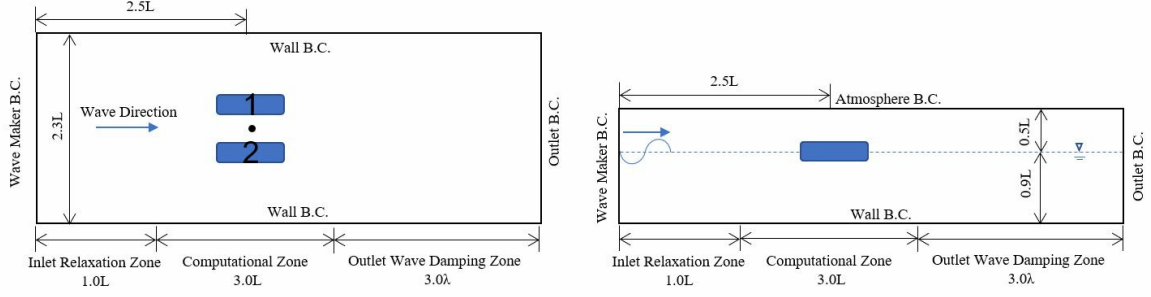
Figure 2: Computational Domain

Time series for heave motion of Body 1, pitch motion of Body 2, and wave elevation at the center of the gap for incident waves ($\lambda/L = 1.69$) along with their comparisons with experimental results are presented in Fig. 3.
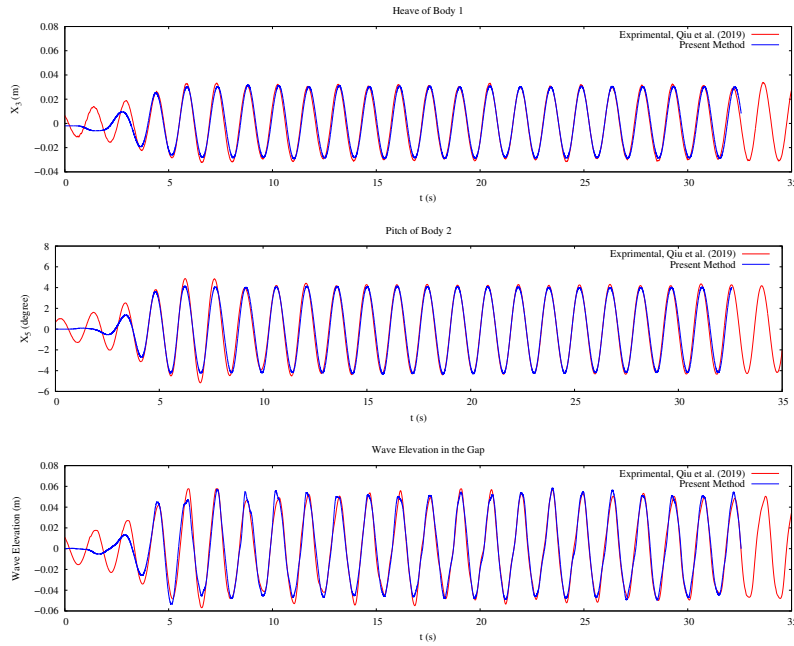
Figure 3: Ship Motions and Wave Elevation for Incident Waves, $\lambda/L = 1.69$

It can be seen that numerical solutions and the experimental data are in good agreement. Time series for heave motion of Body 2, pitch motion of Body 1, and wave elevation at the center of the gap for the shorter incident wave ($\lambda/L = 0.60$) as well as their comparisons with experimental data are presented in Fig. 4.

Compared to the long wave case, greater nonlinearity in experimental and numerical results is observed. The numerical results agree well with the experimental data, except that the heave motion is slightly under predicted. Further investigation on the under-prediction is being carried out by increasing the grid resolution.

4 Conclusion

An FVM code with the immersed boundary method has been developed to simulate two-body interactions in waves. The velocity boundary conditions on immersed boundaries are satisfied more accurately as they are enforced in the pressure-velocity coupling. A geometrical VOF method is employed to model the free surface and to maintain the sharpness of interface and the conservation of mass. The predicted body motions and wave elevations in the gap are in good agreement with the experimental data.
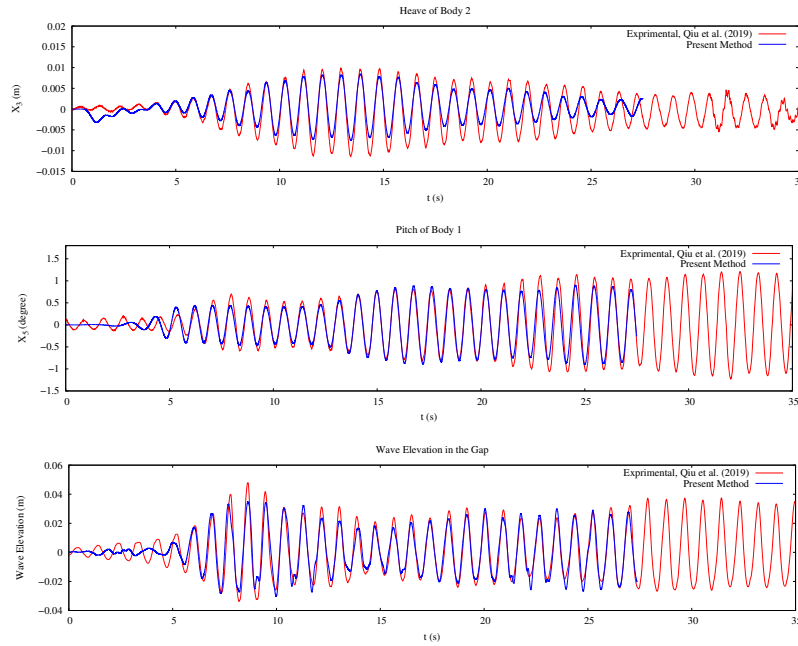
Figure 4: Ship Motions and Wave Elevations for Incident Waves, $\lambda/L = 0.60$

Acknowledgement

References

Chen, X., 2004, Hydrodynamics in Offshore and Naval Applications - Part I, 6th International Conference on Hydrodynamics, Perth, Australia.

Huijsmans, R.H.M., Pinkster, J.A. and de Wilde, J.J., 2001, Diffraction and Radiation of Waves around Side-by-Side Moored Vessels, 11th International Offshore and Polar Engineering Conference, Maui, Hawaii, USA.

Jacobsen, N.G., Fuhrman, D.R. and Fredsøe, J., 2012, A Wave Generation Toolbox for the Open-Source CFD Library: OpenFoam, International Journal for Numerical Methods in Fluids, Vol. 70, No. 9, pp. 1073-1088.

Newman, J.N., 2003, Application of Generalized Models for the Simulation of Free Surface Patches in Multi Body Hydrodynamics, WAMIT Consortium Report.

Ok, H., Lee, S.J., Choi, J.H., 2017, Numerical Simulation of Motion of Single and Side-by-Side Vessels in Regular waves Using Openfoam, Ships Offshore Structures, Vol. 12, No. 6, pp. 793–803.

Qiu, W., Meng, W., Peng, H., Li, J., Rousset, J.M., Rodríguez, C.A., 2019, Benchmark Data and Comprehensive Uncertainty Analysis of Two-body Interaction Model Tests in a Towing Tank, Ocean Engineering, Vol. 171, pp.663-676.

Roenby, J., Bredmose, H, and Jasak, H., 2016, A Computational Method for Sharp Interface Advection, Royal Society Open Science, Vol. 3, No. 1.